



Identification and further development of thiazolidinones spiro-fused to indolin-2-ones as potent and selective inhibitors of *Mycobacterium tuberculosis* protein tyrosine phosphatase B

Viktor V. Vintonyak^a, Karin Warburg^{a,b}, Björn Over^{a,b}, Katja Hübel^a, Daniel Rauh^{b,c}, Herbert Waldmann^{a,b,*}

^a Max-Planck-Institute of Molecular Physiology, Otto-Hahn-Strasse 11, D-44227 Dortmund, Germany

^b Technische Universität Dortmund, Chemical Biology, Otto-Hahn-Strasse 6, D-44227 Dortmund, Germany

^c Chemical Genomics Centre of the Max Planck Society, Otto-Hahn-Strasse 15, D-44227 Dortmund, Germany

ARTICLE INFO

Article history:

Received 15 February 2011

Received in revised form 4 April 2011

Accepted 7 April 2011

Available online 14 April 2011

Keywords:

Chemical biology
Enzyme inhibitors
Medicinal chemistry
Molecular modeling

ABSTRACT

Tuberculosis continues to be a major cause of morbidity and mortality throughout the world. Protein tyrosine phosphatases from *Mycobacterium tuberculosis* are attractive targets for developing novel strategies in battling tuberculosis due to their role in the intracellular survival of *M. tuberculosis* in various infection models. Here, we report on the identification and further development of thiazolidinones spiro-fused to indolin-2-ones as a new class of potent and selective inhibitors of *M. tuberculosis* protein tyrosine phosphatase B. Detailed structure–activity relationship (SAR) studies revealed that a nitro-substituted 2-oxindole core together with a dihalogenated anilide and a halogenated *N*-benzyl moiety are essential for strong inhibitory activity against MptpB (*M. tuberculosis* protein tyrosine phosphatase B). Small structural modification of the identified compounds led to significant improvement of compound solubility and cell permeability retaining inhibitory activity in the micromolar range. The configuration of the spiro-center was found to be crucial for the inhibitory activity and the separation of the racemate revealed the *R*-(–)-enantiomers as the biologically active component. The reported MptpB inhibitors show excellent selectivity against a selected panel of protein tyrosine phosphatases, including MptpA (*M. tuberculosis* protein tyrosine phosphatase A), PTP1B (protein tyrosine phosphatase 1B), SHP-2 (Src homology 2 domain-containing protein tyrosine phosphatase), PTPN2, h-PTP β (human protein tyrosine phosphatase β), and VHR (*Vaccinia virus* VH1-related dual-specific protein phosphatase) and further highlight the identified thiazolidinones spiro-fused to indolin-2-ones as a promising class of new compounds that might prove useful for chemical biology research to dissect MptpB function and eventually foster the development of next generation antibiotics.

© 2011 Elsevier Ltd. All rights reserved.

1. Introduction

Tuberculosis (TB) continues to be a major cause of morbidity and mortality throughout the world. According to the World Health Organization, one-third of the world's population is infected with *Mycobacterium tuberculosis* and about 35 million people are expected to die from TB in the first 20 years of this century.¹ Because of the increasing occurrence of drug-resistant mycobacteria and the need of the extended use of current drugs, new targets and drugs for therapeutic interventions are in high demand. *M. tuberculosis* protein tyrosine phosphatase A (MptpA) and MptpB are two enzymes secreted by growing mycobacteria and believed to mediate *M. tuberculosis* survival in macrophages by dephosphorylation

of host proteins that are involved in the interferon signaling, which represents a crucial pathway of the immune system.² The genetic knock-out of MptpB suppresses growth of *M. tuberculosis* in activated macrophages and guinea pigs and suggests that MptpA/B could qualify as potential drug targets in the treatment of TB.³ The importance of MptpB to the intracellular survival of *M. tuberculosis* was recently confirmed by two independent studies in which specific inhibitors directed against MptpB were shown to impair mycobacterial survival in murine macrophages.⁴ Since MptpB has no direct human orthologues, inhibitors active against MptpB might not only prove useful as probe molecules in chemical biology research to dissect the functional role of phosphatases in cell invasion, but also offer unique opportunities for the development of new antitubercular drugs.

Compounds with anti MptpA and MptpB activity have been successfully identified and characterized in vitro.⁵ In particular, the

* Corresponding author. Tel.: +49 (0) 231 133 2400; fax: +49 (0) 231 133 2499; e-mail address: herbert.waldmann@mpi-dortmund.mpg.de (H. Waldmann).

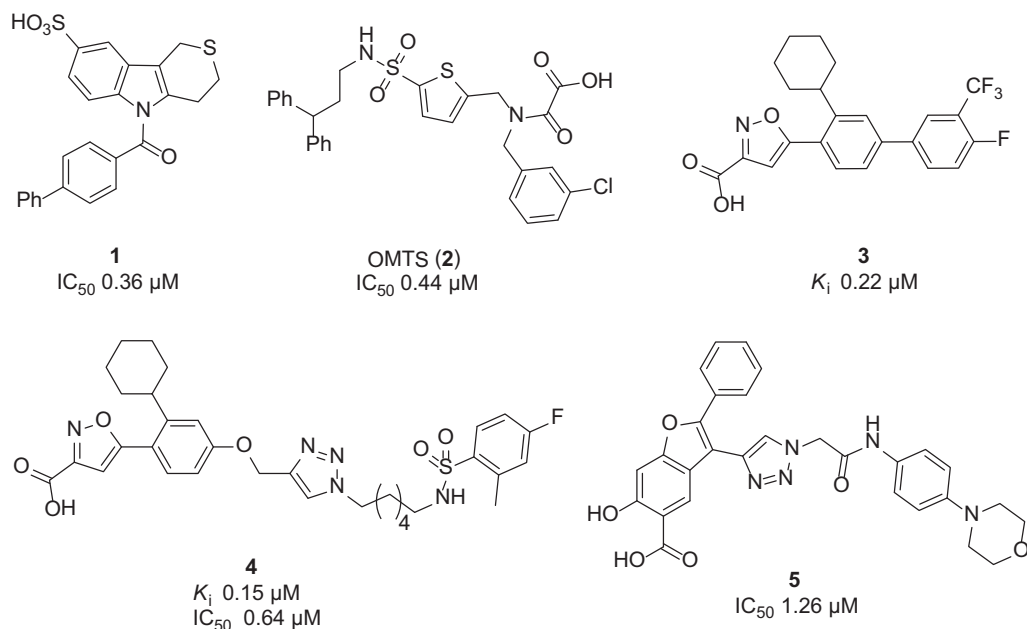


Fig. 1. Structures of selected MptpB inhibitors, IC_{50} or K_i values are given.

application of biology-oriented synthesis (BIOS) approaches resulted in the identification of indole derivative **1** (Fig. 1), as potent and specific inhibitor of MptpB.⁶ Recently Alber et al. reported the development of a potent and selective (oxalylamino-methylene)-thiophene sulfonamide inhibitor for MptpB (**2**) (OMTS).⁷ Compound **2** shows an IC_{50} value of 440 ± 50 nM and >60 -fold selectivity for MptpB over six human PTPs. Application of a substrate-based fragment approach resulted in the discovery of the isoxazole **3**, which is one of the most potent MptpB inhibitors known from literature to date (K_i of 220 nM).⁸ Using the structure of isoxazole **3** as a starting point, Yao et al. recently synthesized and screened a click chemistry-based library of MptpB inhibitors and identified **4** as the most active representative with a K_i value of 0.15 μ M for MptpB but only moderate selectivity when screened against PTP1B, TCPTP (T-cell protein tyrosine phosphatase), Yop-H (*Yersinia* protein tyrosine phosphatase), and LMW-PTP (low molecular weight protein tyrosine phosphatase).⁹ Recently Zhou et al. identified a potent and selective MptpB inhibitor **5** with significant cellular activity, from a combinatorial library of bidentate benzofuran salicylic acid derivatives assembled by click chemistry.^{4b}

Remarkably, the aforementioned inhibitors all contain highly polar acidic groups that are highly ionized at physiologic pH and

can be expected to display exceedingly poor cell permeability and low oral bioavailability. Indeed, compound **4** is not cell permeable or its cell permeability cannot be determined.⁹ After all, the discovery of potent cell permeable and orally bioavailable MptpB inhibitors is a challenging task of medicinal chemistry research. New inhibitor classes with good selectivity profiles and improved pharmacological properties are therefore in high demand.

Recently we communicated on the identification of the indolin-2-on-3-spirothiazolidinones as a novel class of potent and selective inhibitors of MptpB.¹⁰ In the present study we present detailed systematic structure–activity relationship (SAR) studies, investigations of the inhibition profiles, and biochemical evaluation toward the mode of action of the early discovered compounds as well as molecular docking study.

2. Results and discussion

Using enzyme activity assays we screened a library of 40,000 compounds to discover inhibitors of MptpB.^{6a} In a 384-well HTS format we used *p*-nitrophenyl phosphate (*p*-NPP) as the substrate and identified **6–9** as a series of compounds that perturbed substrate hydrolysis by MptpB in the mid-micromolar range (Fig. 2).

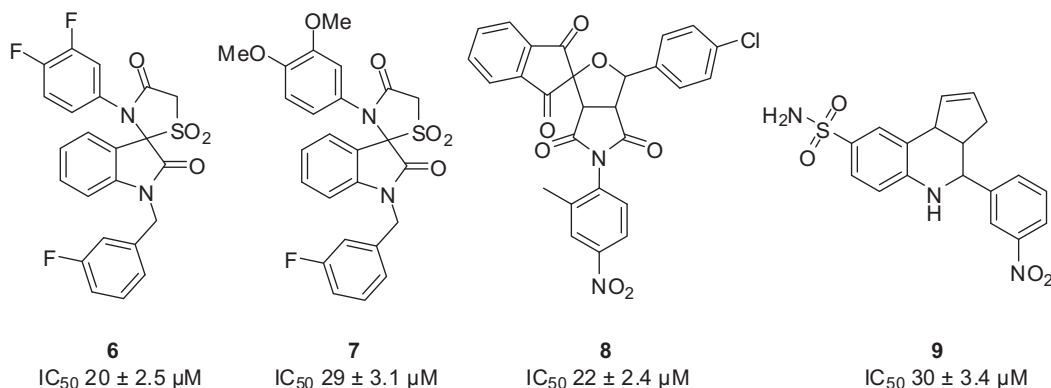


Fig. 2. Structures and IC_{50} values of primary hits derived from HTS against MptpB.

Interestingly, **6** and **7** showed excellent selectivity against a selected panel of PTP (Cdc25A, PTP1B, MptpA, VHR, PP1 (protein phosphatase 1), SHP-2, VE-PTP (vascular endothelial protein tyrosine phosphatase), PTPN2) and, to the best of our knowledge, were not reported as phosphatase inhibitors before. Moreover, **6** and **7** contain a 2-oxindole moiety, which is found in a large number of natural products with broad spectrum biological activity. We concluded that these compounds might represent biologically prevalidated starting points for further compound development as their underlying scaffolds were most likely selected by evolution as suitable core structures for protein binding.^{11,12} We focused on the indolin-2-on-3-spirothiazolidinone scaffold to develop further compound libraries with improved affinities and to investigate the relevance of the configuration of the spiro-center for biological activity.

2.1. Design and synthesis of first generation library based on the primary hits

Given the moderate activities of the identified primary hits **6** and **7** in inhibiting phosphatase activity, we set out to improve potency against MptpB and to obtain proper SAR of the newly identified inhibitor scaffold. We followed a classical medicinal chemistry approach and identified the anilide substituent of the thiazolidinone, the *N*-alkyl substituent on the 2-oxo-indole as well as the thiazolidinone moiety and the 2-oxo-indole inhibitor core as suitable positions for chemical modifications (Fig. 3).

Our synthesis commenced with the alkylation of commercially available 1*H*-indole-2,3-diones **10** and **10a** with different alkyl and benzyl halides and provided a small focused library of *N*-substituted isatins **11** and **15** (Scheme 1). Condensation of **11** and **15** and the unprotected isatin **10** with various anilines resulted in the formation of isatin-3-imines, which subsequently were directed to cyclocondensation with mercaptoacetic acid to provide substituted

indolin-2-on-3-spirothiazolidinones **12**, **16**, and **17**. The obtained sulfides **12**, **16**, and **17** were readily oxidized to the corresponding sulfones **13**, **18**, and **19** with 5 equiv of *m*CPBA. Remarkably, the reaction of **12ac** with a slight excess of *m*CPBA (1.1 equiv) in CHCl₃ at 0 °C resulted in exclusive formation of sulfoxide **14** as a single diastereomer (*dr*>20:1). In order to improve the solubility of the final compounds, the *tert*-butyl ester of **19b** was removed and the obtained acid **20** was subsequently coupled to different aliphatic amines using standard techniques to provide the corresponding amides **21a–d** in excellent yield.

2.2. In vitro characterization of first generation substituted indolin-2-on-3-spirothiazolidinone

To explore how chemical modifications of the indolin-2-on-3-spirothiazolidinones are tolerated by MptpB, we measured enzyme inhibition by using *p*-NPP as the substrate and observing the release of *p*-nitrophenol at 405 nm (Table 1). We observed a significant (up to 23-fold) increase in potency in the measured IC₅₀ values when compared to the primary screening hits **6** and **7**. Briefly, the kinetics clearly demonstrate that (a) the halogenated *N*-benzyl substituent on the 1-position of the oxindole is needed to retain activity while (b) a nitro group in the 5-position of the oxindole core significantly enhances potency against MptpB.

One of the trends observed in the indolin-2-on-3-spirothiazolidinone series was the crucial role of the substituted *N*-benzyl fragment for activity against MptpB (Table 1). Compounds lacking any substituent at the 2-oxindole nitrogen (**18a–f**) or bearing aliphatic alkyl groups (**19**, **20**, and **21**) were inactive. Another important trend was observed for substituents in the 2-oxindole core. Much to our surprise, the introduction of a nitro group in the 5-position of 2-oxindole core (**13y**) enhanced potency (17-fold) against MptpB while its replacement with a methoxy (**13z**) or

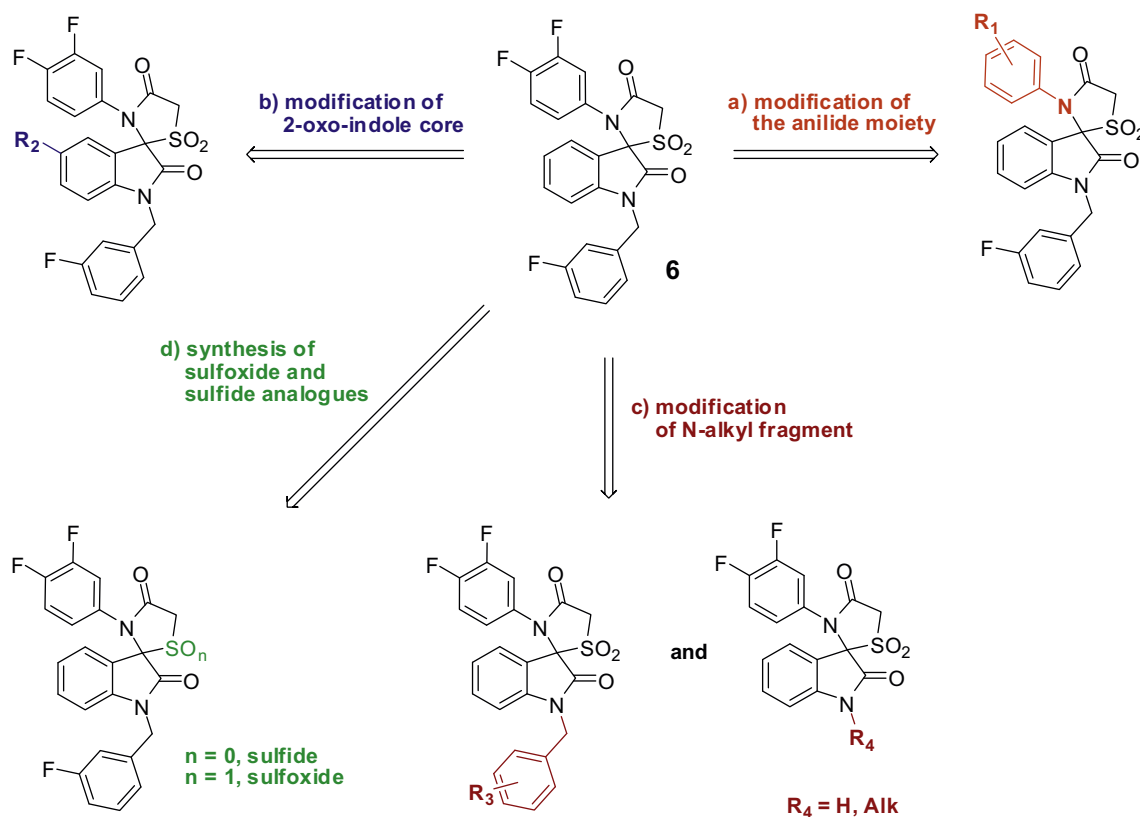
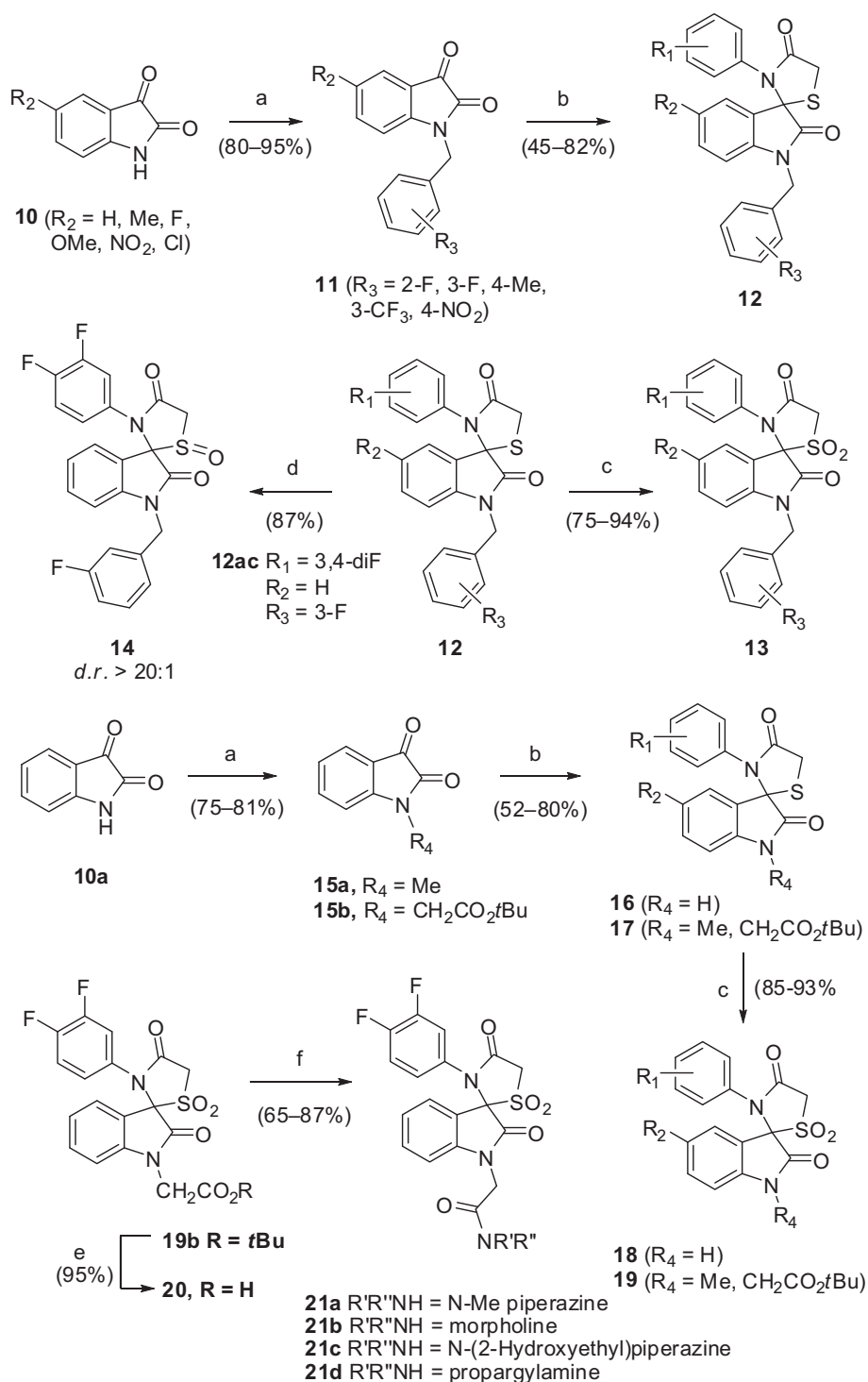


Fig. 3. Potential positions for modification of primary hit **6**.



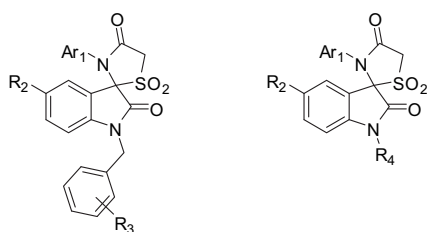
Scheme 1. Preparation of the first generation library based on the primary hit **6**. Reagents and conditions: (a) NaH, DMF, 0 °C, then ArCH₂Br or Alk-Hal; (b) (1) ArNH₂, EtOH, reflux, 6 h; (2) mercaptoacetic acid, toluene, reflux, 16 h; (c) mCPBA (5 equiv), CHCl₃, rt, 24 h; (d) mCPBA (1.1 equiv), CHCl₃, 0 °C, 1 h; (e) TFA, DCM, 0 °C, 2 h; (f) R'R''NH, HBTU, HOBT, DIPEA, DMF.

methyl group (**13aa**) resulted in inactive compounds. Additionally, the halide substitution pattern of the anilide fragment turned out to be important as well. Compounds possessing two fluorine or fluorine and chlorine atoms in the *meta*- and *para*-position of the anilide fragment (**6**, **13g**, **13o**, **13x**, **13y**, and **13ab**) are preferred over analogues bearing mono- (**13a–d**, **13h**, **13n**, and **13w**) or dialkylsubstituents. The sulfide intermediate **12** did not show any inhibitory activity, while sulfoxide **14** (IC₅₀, 13.3 μM) was almost twice as active, as the corresponding sulfone **6**.

2.3. Synthesis of the second generation indolin-2-on-3-spirothiazolidinones

To build on the initial SAR of indolin-2-on-3-spirothiazolidinone substituted at the 1- and 3'-positions and the finding that a nitro group at the 5-position is crucial for affinity, we set out to further explore this position. For this purpose, carbomethoxy, sulfonamide, and trifluoromethoxy groups were chosen. Substituted isatins **25–30** were prepared as illustrated in Scheme 2. Preparation of **24a**

Table 1
 IC₅₀ values of indolin-2-on-3-spirothiazolidinones are shown for MptpB^a



Compd	Ar ₁	R ₂	R ₃ or R ₄	IC ₅₀ , μM	Compd	Ar ₁	R ₂	R ₃ or R ₄	IC ₅₀ , μM
6		H	R ₃ =3-F	20.0±2.5	13v		H	R ₃ =3-F	n.a.
7		H	R ₃ =3-F	29.0±3.1	13w		H	R ₃ =3-F	n.a.
13a		H	R ₃ =4-Me	n.a.	13x		H	R ₃ =4-NO ₂	22.4±1.8
13b		H	R ₃ =4-Me	n.a.	13y		NO ₂	R ₃ =3-F	1.2±0.2
13c		H	R ₃ =2-F	n.a.	13z		OMe	R ₃ =3-F	n.a.
13d		H	R ₃ =3-CF ₃	n.a.	13aa		Me	R ₃ =3-F	n.a.
13e		H	R ₃ =3-F	32.8±2.4	13ab		Cl	R ₃ =4-NO ₂	21.1±3.1
13f		H	R ₃ =3-F	35.5±3.3	14^b		H	R ₃ =3-F	13.3±2.2
13g		H	R ₃ =3-F	22.8±2.7	18a		H	R ₄ =H	n.a.
13h		H	R ₃ =3-F	n.a.	18b		H	R ₄ =H	n.a.
13i		H	R ₃ =3-F	n.a.	18c		H	R ₄ =H	n.a.
13j		H	R ₃ =3-F	29.4±2.1	18d		OMe	R ₄ =H	n.a.
13k		H	R ₃ =3-F	n.a.	18e		F	R ₄ =H	n.a.
13l		H	R ₃ =3-F	n.a.	18f		NO ₂	R ₄ =H	n.a.

(continued on next page)

Table 1 (continued)

Compd	Ar ₁	R ₂	R ₃ or R ₄	IC ₅₀ , μM	Compd	Ar ₁	R ₂	R ₃ or R ₄	IC ₅₀ , μM
13m		H	R ₃ =3-F	n.a.	19a		H	R ₄ =Me	n.a.
13n		H	R ₃ =3-F	n.a.	19b		H		n.a.
13o		H	R ₃ =4-Me	27.4±3.7	19c		H	R ₄ =Me	n.a.
13p		H	R ₃ =3,4-diF	22.5±1.9	19d		H	R ₄ =Me	n.a.
13q		H	R ₃ =3-F	28.0±3.1	20		H		n.a.
13r		H	R ₃ =3-F	24.8±2.2	21a		H		n.a.
13s		H	R ₃ =3-CF ₃	32.2±3.2	21b		H		n.a.
13t		H	R ₃ =2-F	33.0±2.8	21c		H		n.a.
13u		F	R ₃ =3-F	n.a.	21d		H		n.a.

n.a.=not active (no inhibition up to a concentration of 100 μM).

^a All IC₅₀ values were calculated from at least three independent measurements.

^b Sulfoxide.

was started from ethyl 4-aminobenzoate **22a** using reported procedures.¹³ α -Isonitrosoacetanilide, obtained by reaction of ethyl 4-aminobenzoate, hydroxylamine hydrochloride and chloral hydrate, was subsequently cyclized into isatin-5-carboxylic acid **23a** and the carboxylic function was then transformed into the corresponding methyl ester **24a**. In a similar way, starting with 4-aminobenzenesulfonamide **22b** isatin **23b** could be prepared in respectable yield. In order to enlarge our building blocks library, commercially available isatins **10** as well as synthesized derivatives **23b** and **24a** were alkylated with different benzyl bromides. Methoxy substituted derivatives **27** were selected for further derivatisation. Demethylation mediated by boron tribromide afforded 5-hydroxy isatins **29**, which afterward were subjected to alkylation with *tert*-butyl bromoacetate. The *tert*-butyl group could be easily removed on the final step of the synthesis to provide corresponding hydroxyacetic acid derivatives.

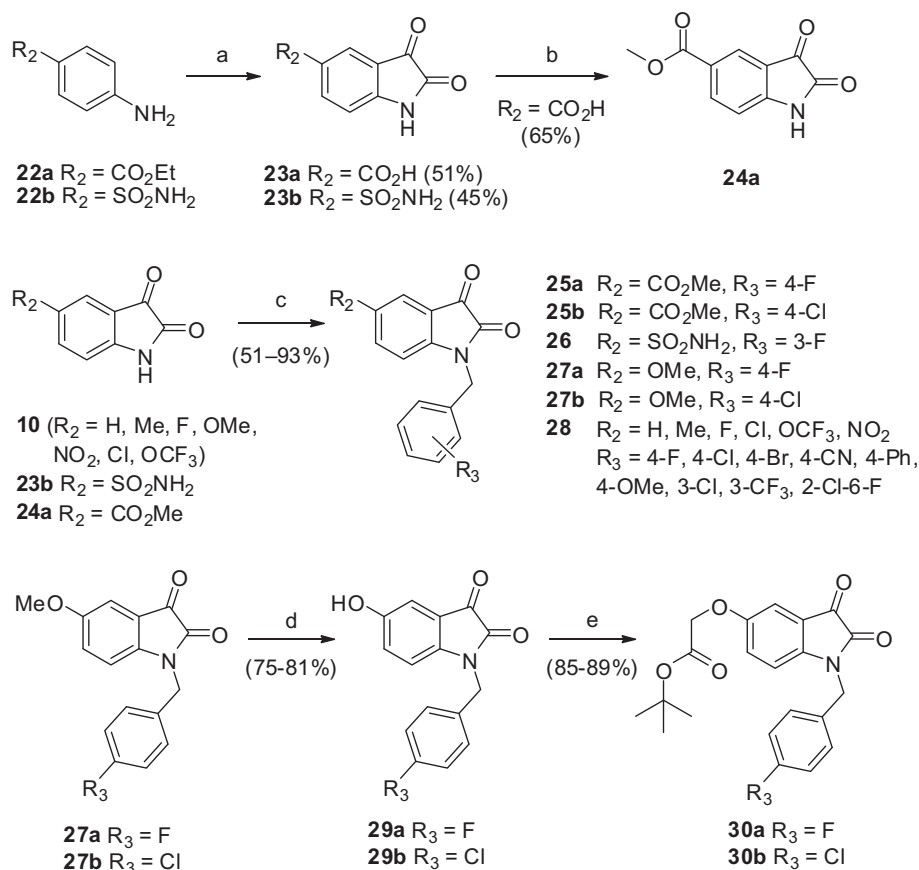
N-Benzylated isatins were then converted into the corresponding isatin-3-imines and subsequently cyclized into indolin-2-on-3-spirothiazolidinone **31–35** following established procedures outlined above. Since the sulfoxide **14** showed higher activity compared to the corresponding sulfone **6**, we decided to further explore this SAR and synthesized a small focused library of sulfoxides. Consequently, the obtained sulfides **31–35** were converted into the corresponding sulfones **36–40** and sulfoxides **41–45**

(Scheme 3). Derivatives **40** and **45**, bearing a *tert*-butyl acetate were subjected to acid mediated deprotection. This transformation delivered carboxylic acids **46** and **47**.

The newly synthesized indolin-2-on-3-spirothiazolidinones **36–47** were investigated for their inhibitory effects on MptpB (Tables 2 and 3).

Our initial SAR (Table 1) showed that introduction of a nitro group into the 5-position of the 2-oxindole core (**13y**, IC₅₀=1.2±0.2 μM) significantly enhances the inhibitory activity. The measured IC₅₀ values for the second generation of compounds further highlight this trend.

We next set out to investigate the role of the substituted *N*-benzyl fragment and synthesized 13 analogues of **13y**, displaying different substituents in the phenyl ring (Scheme 3). IC₅₀ values showed that replacement of the fluorine with chlorine (**39an**) or a trifluoromethyl group (**39ao**) as well as relocation of the fluorine to the *para*-position of the phenyl ring did not improve potency when compared to **13y**. Surprisingly, substitution of the *para*-fluorine with chlorine (**39i**) or bromine (**39ah**) resulted in two and threefold increase in potency and highlight that the strength of the interactions attenuates in the order Br>Cl>F. This observation is perfectly in line with characteristics discovered within small model halogen-bonded systems.¹⁴ Replacement, of the *para*-fluorine with a cyano group (**39al**) was well tolerated and resulted in a slight



Scheme 2. Synthesis of an isatin library. Reagents and conditions: (a) (1) $\text{CCl}_3(\text{OH})_2$, $\text{NH}_2\text{OH}\cdot\text{HCl}$, H_2SO_4 ; (2) $\text{H}_2\text{SO}_4(\text{concd})$, 90°C ; (b) EDC, DMAP, MeOH, rt; (c) NaH, DMF, 0°C , then ArCH_2Br ; (d) BBr_3 , DCM, 0°C ; (e) NaH, DMF, 0°C , then $\text{BrCH}_2\text{CO}_2\text{tBu}$.

improvement in potency when compared to **39g**. On the other hand, introduction of *para*-hydroxy (**39ai**) and methoxy groups (**39ag**) resulted in a two to sixfold decrease in activity. Notably, the replacement of the *N*-benzyl fragment by 5-methylisoxazole (**39av**) was tolerated but did not improve potency of the compound when compared to **39g**. To further explore the role of the dihalogenated anilide fragment for MptpB inhibitory activity we synthesized analogues with different substituents in this part of the molecule and found that the substitution of the *meta*-fluorine with chlorine was well tolerated. On the other hand, introduction of alkyl substituents in the anilide moiety resulted in complete loss of inhibitory activity (Table 2). From these results we concluded that a nitro-substituted 2-oxindole core in combination with a dihalogenated anilide moiety, as well as a halogenated *N*-benzyl fragment are prerequisites for strong inhibitory activity against MptpB.

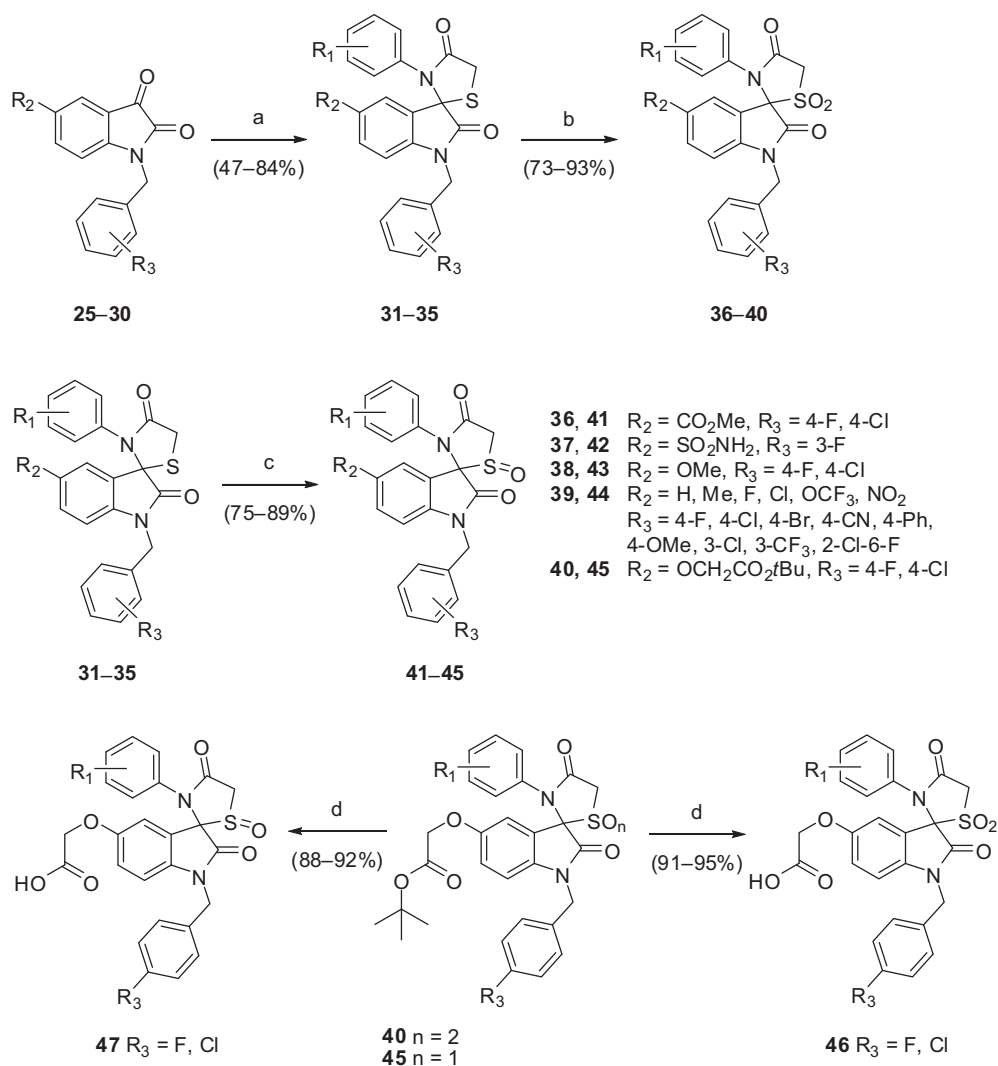
2.4. SAR trends in the sulfoxide series

As a general trend in the sulfoxide series we observed a high tolerance toward the nature of substituents in the anilide moiety and the 2-oxindole core. Similar to the sulfones, the most active sulfoxides possessed a nitro group in the 5-position of the 2-oxindole core and a dihalogenated anilide moiety (Table 3). However, this time derivatives bearing an alkyl-substituted anilide retained activity. Much to our surprise, replacement of the nitro group by an ester, sulfonamide or trifluoromethoxy group but not by a methoxy group was well tolerated in most cases. Similarly, replacement of the nitro group with halogens (F, Cl) or hydroxyacetic acid resulted in a two to threefold decrease in activity. In conclusion and similar to the investigated sulfones, a nitro-substituted 2-oxindole core together with a dihalogenated anilide

moiety and a halogen-substituted *N*-benzyl fragment are essential for high inhibitory activity of the described sulfoxides. Since sulfoxides bearing alkyl residues in *para*-position of the anilide fragment and different polar substituents in the 2-oxindole core also show significant inhibitory activity, one can speculate that such a high tolerance to the nature of substituents in the sulfoxide series is due to the presence of the highly polarized S–O bond, which may play a crucial role as hydrogen bond acceptor to interact with the active site of MptpB. However, further studies to investigate the sulfoxides including co-crystallization experiments with target phosphatases failed due to their instability in solution. We hypothesize that the instability results from ring opening of the thiazolidinone to form the sulfenic acid, which is likely to decompose further.

2.5. Additional SAR study in the sulfone series

To further explore the SAR around the lead structure **13y**, we reduced the nitro group in the 5-position to the resulting amine **48**, which was then converted to the corresponding acetamide **49a** and carbamate **49b** (Scheme 4). In addition, we were interested in determining the role of the amide carbonyl for inhibitory activity against MptpB. To this end, sulfone **13y** was efficiently converted into the corresponding bis-thioamide **50** by refluxing with Lawesson's reagent in toluene. Biological evaluation showed that transformation of the nitro derivative **13y** into its corresponding amine **48**, acetamide **49a**, and carbamate **49b** is not tolerated by MptpB and leads to a decrease in activity (Table 4). We attribute the moderate activity of the thioamide derivative **50** to the importance of carbonyl groups in **13y**, which may serve as hydrogen bond acceptors.



Scheme 3. Preparation of the second generation indolin-2-on-3-spirothiazolidinones library. Reagents and conditions: (a) (1) ArNH_2 , EtOH, reflux, 6 h; (2) mercaptoacetic acid, toluene, reflux, 16 h; (b) *m*CPBA (5 equiv), CHCl_3 , rt, 24 h; (c) *m*CPBA (1.1 equiv), CHCl_3 , 0 °C, 1 h; (d) TFA, DCM, 0 °C, 2 h.

In order to improve the physicochemical properties of our inhibitors we decided to introduce a carboxylic group into the thiazolidinone ring system. Condensation of isatins **28** with 3,4-difluoroaniline delivered isatin-3-imines, which afterward were directly subjected to cyclocondensation with mercapto-succinic acid to provide substituted spiro[indoline-3,2'-thiazolidine]-2,4'-diones **51**. In order to avoid difficulties during purification we replaced *m*CPBA by Oxone[®] in the oxidation step.¹⁵

All synthesized compounds were evaluated for inhibitory activity against MptpB (Tables 4 and 5). In addition, sulfones **13y**, **39av**, **39g**, **39l**, **39ah**, **39an**, **39ao** and the acetic acid containing analogue **52**, were subjected to PAMPA (parallel artificial membrane permeability) assays to determine cell membrane permeability.

Introduction of a carboxylic function into the thiazolidinone ring does not alter biological activity and significantly increases compound solubility and cell permeability. Remarkably, despite relatively moderate solubility (103 μM), sulfone **39av** shows excellent cell permeability (46%).

2.6. Separation of enantiomers

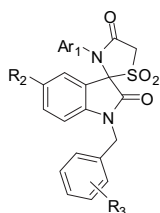
All indolin-2-on-3-spirothiazolidinone discussed above were synthesized as racemates. In order to shed light onto the relevance

of the configuration of the spiro-center on the inhibitory activity against MptpB, we separated the 10 most potent sulfones into their pure enantiomers by means of preparative high-performance liquid chromatography with chiral stationary phase (see [Experimental section](#) for details) and determined their IC_{50} values (Table 6).

In all cases the (*R*)-(-)-enantiomers were 10–20 times more potent than their corresponding (*S*)-(+)-antipodes. The most active compounds displayed IC_{50} values in the nanomolar range (Table 6). The absolute configuration was assigned using combination of experimental circular dichroism (CD) investigations with quantum chemical CD calculations.¹⁰

2.7. Synthesis of structural analogues in order to determine the binding mode

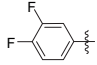
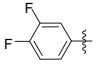
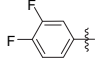
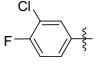
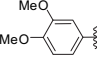
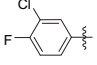
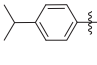
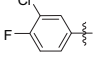
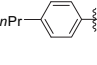
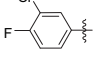
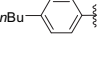
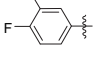
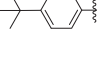
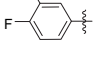
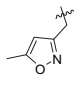
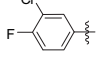
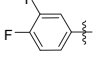
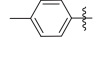
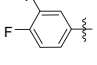
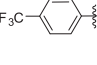
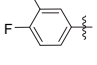
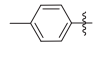
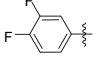
One of the key structural features of the indolin-2-on-3-spirothiazolidinones is the presence of highly acidic methylene protons in the thiazolidinone ring. This position is activated by both the carbonyl and the sulfone/sulfoxide function, respectively. In polar solvents one can assume rapid formation of an equilibrium between the 'amide'- (**A**) and 'enol'-form (**B**) (with a shift in favor of the 'amide'-form **A**) (Fig. 4). We hypothesized, that due to its acidic nature, the 'enol'-form (**B**) might play a crucial role in recognizing

Table 2IC₅₀ values of indolin-2-on-3-spirothiazolidinones are shown for MptpB^a

Compd	Ar ₁	R ₂	R ₃	IC ₅₀ , μM	Compd	Ar ₁	R ₂	R ₃	IC ₅₀ , μM
36a		CO ₂ Me	4-F	18.1±2.1	39x		NO ₂	4-F	n.a.
36b		CO ₂ Me	4-Cl	14.7±1.7	39y		NO ₂	4-F	6.5±1.0
37		SO ₂ NH ₂	4-F	16.4±1.9	39z		NO ₂	4-F	n.a.
38a		OMe	4-F	n.a.	39aa		NO ₂	4-F	30.5±2.4
38b		OMe	4-F	22.1±2.1	39ab		NO ₂	4-F	13.7±1.8
38c		OMe	4-Cl	24.2±2.3	39ac		H	4-F	n.a.
39a		NO ₂	4-F	n.a.	39ad		NO ₂	4-Br	1.8±0.4
39b		F	4-F	n.a.	39ae		OCF ₃	4-F	22.3±2.4
39c		Me	4-F	n.a.	39af		OCF ₃	4-Cl	20.5±1.9
39d		NO ₂	4-Cl	n.a.	39ag		NO ₂	4-OMe	22.1±2.1
39e		F	4-Cl	n.a.	39ah		NO ₂	4-Br	1.1±0.3
39f		H	4-F	32.3±2.1	39ai		NO ₂	4-OH	8.2±1.9
39g		NO ₂	4-F	3.6±0.8	39aj		NO ₂	3,4,5-Tri-F	6.4±0.8
39h		F	4-F	27.7±2.3	39ak		NO ₂	3,4-Di-F	4.8±0.5
39i		Me	4-F	n.a.	39al		NO ₂	4-CN	3.1±0.4
39j		Cl	4-F	28.5±2.5	39am		NO ₂	2-Cl, 6-F	7.5±0.7
39k		H	4-Cl	29.7±3.2	39an		NO ₂	3-Cl	2.1±0.6
39l		NO ₂	4-Cl	1.8±0.4	39ao		NO ₂	3-CF ₃	3.2±0.5

(continued on next page)

Table 2 (continued)

Compd	Ar ₁	R ₂	R ₃	IC ₅₀ , μM	Compd	Ar ₁	R ₂	R ₃	IC ₅₀ , μM
39m		F	4-Cl	24.2±2.8	39ap		NO ₂	4-Ph	19.8±1.5
39n		Cl	4-Cl	28.0±2.2	39aq		NO ₂	3-Cl	2.7±0.4
39o		H	4-F	n.a.	39ar		NO ₂	3,4,5-Tri-F	4.7±0.4
39p		H	4-F	n.a.	39as		NO ₂	3,4-Di-F	3.3±0.3
39q		H	4-F	n.a.	39at		NO ₂	3-CF ₃	3.9±0.8
39r		H	4-F	27.7±1.9	39au		NO ₂	4-Cl	2.7±0.7
39s		H	4-F	n.a.	39av		NO ₂		4.0±0.4
39t		H	4-F	29.3±2.3	40a		OCH ₂ -CO ₂ Bu	4-Cl	31.4±2.7
39u		H	4-F	28.2±2.5	40b		OCH ₂ -CO ₂ Bu	4-F	n.a.
39v		H	4-F	n.a.	46a		OCH ₂ -CO ₂ H	4-Cl	20.9±1.9
39w		NO ₂	4-F	18.4±2.1	46b		OCH ₂ -CO ₂ H	4-F	22.5±2.4

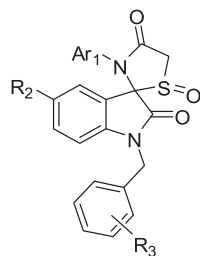
Bold values represents highlight IC₅₀ values < 10 μM.

n.a.=not active (no inhibition up to a concentration of 100 μM). We observed that replacement of the nitro group by methyl ester (**36a,b**), sulfonamide (**37**), methoxy (**38b,c**) or trifluoromethoxy (**39ae,af**) groups led to loss of inhibitory activity. Introduction of halogens (**39h,j**), methyl groups (**39i**), and hydroxyacetate residues (**40a,b**, **46a,b**) into the 2-oxindole core had a detrimental effect on the inhibitory activity. The obtained analogues displayed the same or even lower activity compared to the unsubstituted sulfone **6**. From the above in vitro data it can be concluded that the nitro-substituted 2-oxindole fragment is essential for the high inhibitory activity against MptpB.

^a All IC₅₀ values were calculated from at least three independent measurements.

Table 3

IC₅₀ values of indolin-2-on-3-spirothiazolidinones are shown for MptpB^a



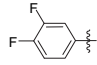
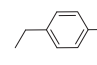
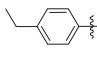
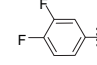
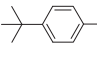
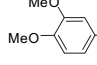
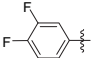
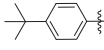
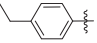
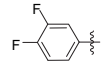
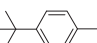
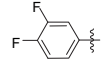
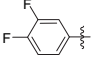
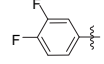
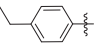
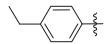
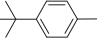
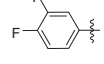
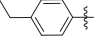
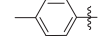
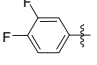
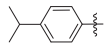
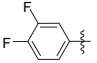
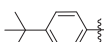
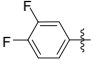
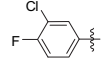
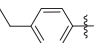
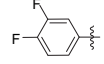
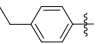
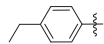
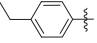
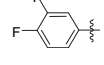
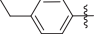
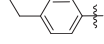
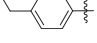
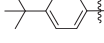
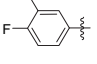
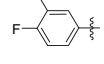
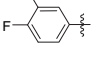
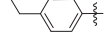
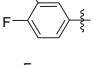
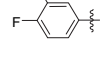
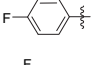
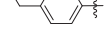
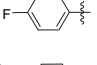
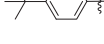
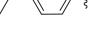
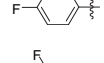
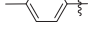
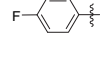
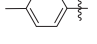
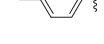
Compd	Ar ₁	R ₂	R ₃	IC ₅₀ , μM	Compd	Ar ₁	R ₂	R ₃	IC ₅₀ , μM
41a		CO ₂ Me	4-F	6.0±1.0	44q		Cl	4-Cl	7.6±1.2
41b		CO ₂ Me	4-F	5.6±1.1	44r		Cl	4-Cl	8.9±1.4
41c		CO ₂ Me	4-F	4.5±0.6	44s		H	4-F	n.a.

Table 3 (continued)

Compd	Ar ₁	R ₂	R ₃	IC ₅₀ , μM	Compd	Ar ₁	R ₂	R ₃	IC ₅₀ , μM
41d		CO ₂ Me	4-Cl	5.1±0.5	44t		H	4-F	12.7±1.6
41e		CO ₂ Me	4-Cl	5.5±1.5	44u		H	4-Me	25.9±2.1
41f		CO ₂ Me	4-Cl	6.2±0.9	44v		F	3-F	25.0±2.7
42a		SO ₂ NH ₂	4-F	6.9±1.6	44w		H	2-F	30.2±2.6
42b		SO ₂ NH ₂	4-F	8.3±2.4	44x		H	3-F	27.5±2.4
42c		SO ₂ NH ₂	4-F	3.1±0.7	44y		H	4-NO ₂	18.2±2.3
43a		OMe	4-Cl	14.1±2.2	44z		NO ₂	4-Cl	5.4±0.8
43b		OMe	4-F	21.0±2.5	44aa		NO ₂	4-Cl	2.9±0.5
43c		OMe	4-Cl	18.3±1.8	44ab		NO ₂	4-Cl	1.5±0.4
43d		OMe	3-F	24.0±2.1	44ac		NO ₂	4-Cl	2.2±0.3
44a		H	4-F	10.5±1.3	44ad		NO ₂	4-Br	2.6±0.5
44b		NO ₂	4-F	2.7±0.8	44ae		NO ₂	4-Br	3.8±0.5
44c		F	4-F	10.9±1.3	44af		OCF ₃	4-F	6.1±0.7
44d		H	4-Cl	22.1±2.3	44ag		OCF ₃	4-F	13.1±0.5
44e		NO ₂	4-Cl	3.1±0.6	44ah		NO ₂	4-F	1.4±0.4
44f		H	4-F	26.1±2.2	44ai		NO ₂	4-OMe	9.3±0.9
44g		NO ₂	4-F	5.1±1.1	44aj		NO ₂	4-OMe	14.3±2.6
44h		F	4-F	12.3±1.3	45a		OCH ₂ -CO ₂ Bu	4-F	8.7±0.7
44i		NO ₂	3-F	4.3±0.4	45b		OCH ₂ -CO ₂ Bu	4-F	28.7±2.5
44j		NO ₂	4-Cl	4.5±0.6	45c		OCH ₂ -CO ₂ Bu	4-F	9.2±0.6
44k		H	4-Cl	22.7±2.3	45d		OCH ₂ -CO ₂ Bu	4-Cl	8.3±0.6
44l		NO ₂	4-F	8.7±1.8	47a		OCH ₂ -CO ₂ H	4-F	9.6±0.7
44m		NO ₂	4-F	12.6±1.7	47b		OCH ₂ -CO ₂ H	4-F	8.7±1.1

(continued on next page)

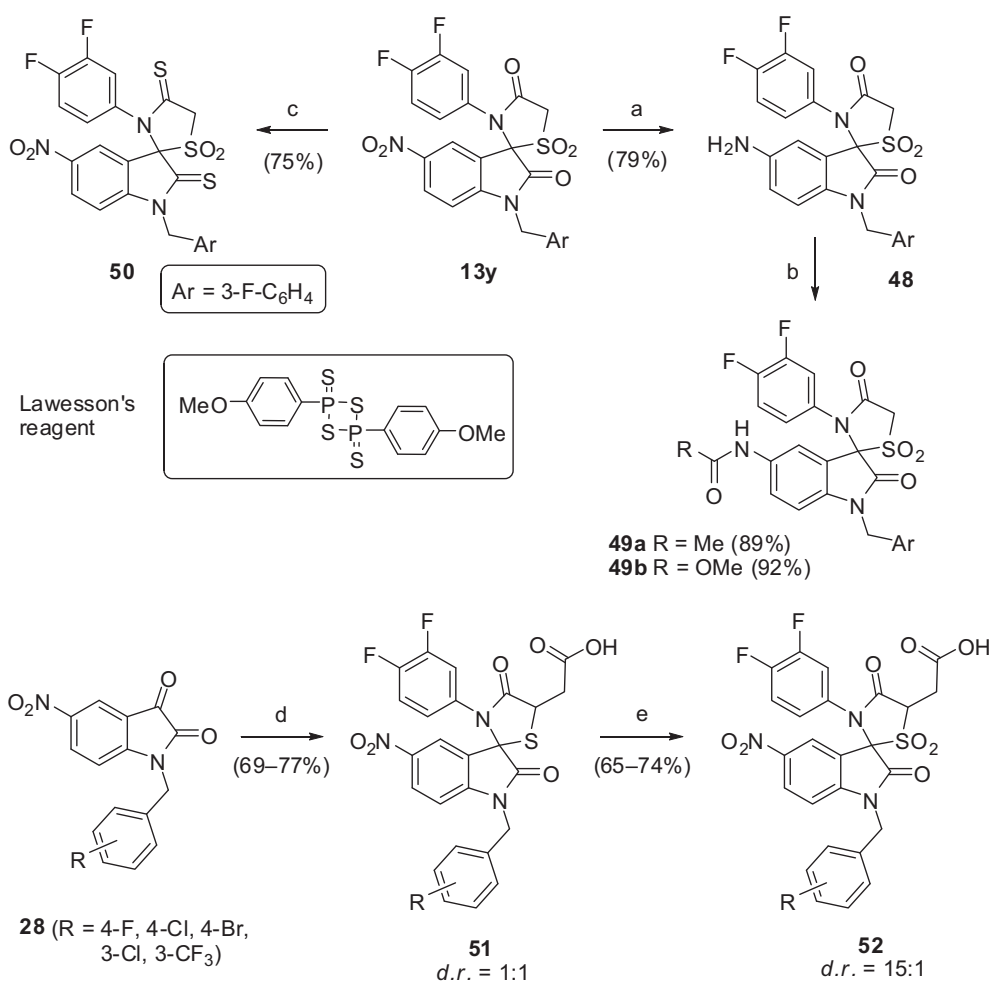
Table 3 (continued)

Compd	Ar ₁	R ₂	R ₃	IC ₅₀ , μM	Compd	Ar ₁	R ₂	R ₃	IC ₅₀ , μM
44n		NO ₂	4-F	4.3±0.5	47c		OCH ₂ -CO ₂ H	4-F	3.9±0.6
44o		NO ₂	4-F	1.5±0.5	47d		OCH ₂ -CO ₂ H	4-Cl	8.2±1.0
44p		NO ₂	4-F	1.2±0.2	47e		OCH ₂ -CO ₂ H	4-Cl	3.0±0.5

Bold values represents highlight IC₅₀ values < 10 μM.

n.a.=not active (no inhibition up to a concentration of 100 μM).

^a All IC₅₀ values were calculated from at least three independent measurements.



Scheme 4. Synthesis of amine **48**, derivatives **49**, **50** and carboxylic acids **52**. Reagents and conditions: (a) HCO₂NH₄, Pd/C, EtOH, reflux, 3 h; (b) RCOCl, pyridine, rt, 12 h; (c) Lawesson's reagent, toluene, reflux, 2 h; (d) 1) 3,4-difluoroaniline, EtOH, reflux, 6 h; (2) mercaptosuccinic acid, toluene reflux, 16 h; (e) Oxone[®] (5 equiv), MeOH/H₂O (1:1), rt, 24 h.

Table 4
IC₅₀ values of spiro[indoline-3,2'-thiazolidine]-2,4'-diones are shown for MptpB^a

Compd	Structural feature	IC ₅₀ , μM
13y	Nitro	1.2±0.2
48	Amine	31.4±2.5
49a	Acetamide	33.1±3.2
49b	Carbamate	34.7±2.8
50	Thioamide	9.6±1.4

Bold values represents highlight IC₅₀ values < 10 μM.

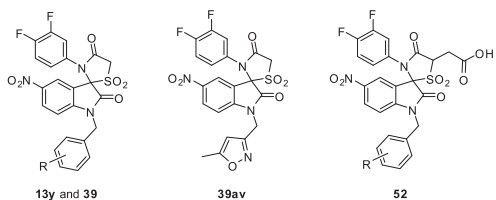
^a All IC₅₀ values were calculated from at least three independent measurements.

the charged active center of the phosphatase. In order to prove this assumption we decided to introduce two methyl groups into the thiazolidinone ring to inactivate tautomerization and to freeze the 'amide'-form.

The synthesis of **53** was straightforward and started with the reaction of isatins **11h**, **28b**, and **28g** with different anilines, followed by cyclocondensation of obtained isatin-3-imines with 2-mercapto-2-methylpropionic acid (Scheme 5). Oxidation of the obtained sulfides delivered the sulfone **53a** and the sulfoxides **53b**, **53c**, and **53d**.

Table 5

IC₅₀ values, solubility, and cell-permeability data of indolin-2-on-3-spirothiazolidinones **13**, **39**, and **52**^a



Compd	R	IC ₅₀ (μM)	Soln ^b (μM)	Compd	R	IC ₅₀ (μM)	Soln ^b (μM)	Flux ^c (%)
13y	3-F	1.2±0.2	157	39av	—	4.0±0.4	103	46
39g	4-F	3.6±0.8	205	52a	4-F	4.8±0.6	430	13
39i	4-Cl	1.8±0.6	225	52b	4-Cl	2.9±0.2	412	20
39ah	4-Br	1.1±0.3	250	52c	4-Br	2.6±0.2	376	20
39an	3-Cl	2.1±0.6	240	52d	3-Cl	2.3±0.2	425	22
39ao	3-CF ₃	3.2±0.4	139	52e	3-CF ₃	2.4±0.3	421	21

Bold values represents highlight IC₅₀ values < 10 μM.

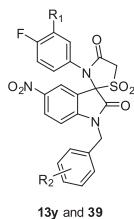
^a All IC₅₀ values were determined from at least three independent measurements.

^b Kinetic solubility as determined by a direct UV assay.¹⁶

^c Cell permeability determined via a parallel artificial membrane permeability assay (PAMPA). Flux (%) denotes concentration (test well)/concentration (control well) × 100.

Table 6

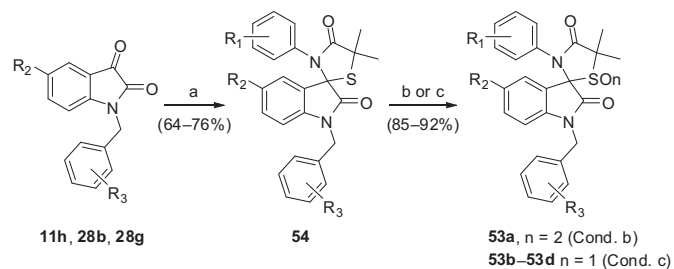
IC₅₀^a values of enantiomerically pure **13y** and **39** are shown for MptpB^a



Compd	R ₁	R ₂	IC ₅₀ , μM.	
			(S)-(+)	(R)-(–)
13y	F	3-F	3.9±0.6	0.32±0.05
39g	F	4-F	5.8±1.1	0.52±0.08
39ah	F	4-Br	2.9±0.5	0.28±0.06
39al	F	4-CN	8.8±0.6	1.3±0.1
39an	F	3-Cl	9.6±1.4	0.94±0.12
39ao	F	3-CF ₃	7.9±0.4	0.38±0.06
39aq	Cl	3-Cl	8.9±0.8	0.51±0.08
39as	Cl	3,4-Di F	11±1.2	1.3±0.2
39at	Cl	3-CF ₃	9.1±0.4	1.4±0.2
39au	Cl	4-Cl	9.5±0.5	1.24±0.15

^a All IC₅₀ values were calculated from at least three independent measurements.

The doubly methylated derivatives **53** showed a complete loss in inhibitory activity when tested against MptpB and highlight that the presence of the 'enol'-form B (Fig. 4) might indeed play a central role possibly as phosphate mimic or to allow for the formation of

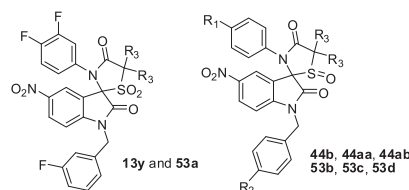


Scheme 5. Synthesis of dimethylated analogues **53**. Reagents and conditions: (a) (1) ArNH₂, EtOH, reflux, 6 h; (2) 2-mercapto-2-methylpropionic acid, toluene, reflux, 16 h; (b) mCPBA (5 equiv), CHCl₃, 0 °C, 1 h; (c) mCPBA (1.1 equiv), CHCl₃, rt, 1 h.

strong hydrogen bonds to surrounding amino acid residues of the active site (Table 7).

Table 7

IC₅₀ values of spiro[indoline-3,2'-thiazolidine]-2,4'-dione are shown for MptpB^a



Compd	R ₁	R ₂	R ₃	IC ₅₀ , μM
53a	NA	NA	Me	n.a.
53b	Et	F	Me	n.a.
53c	<i>i</i> -Pr	Cl	Me	n.a.
53d	<i>t</i> -Bu	Cl	Me	n.a.
13y	NA	NA	H	1.2±0.2
44b	Et	F	H	2.7±0.8
44aa	<i>i</i> -Pr	Cl	H	2.9±0.5
44ab	<i>t</i> -Bu	Cl	H	1.5±0.4

Bold values represents highlight IC₅₀ values < 10 μM.

n.a.=not active (no inhibition up to a concentration of 100 μM).

^a All IC₅₀ values were calculated from at least three independent measurements.

2.8. Determination of the mode of inhibition of MptpB by the identified inhibitors

To gain deeper insight into the mode of MptpB inhibition by the identified spiro-fused indol-2-one-thiazolidinones and to further investigate the proposed role of the 'enol'-form of the thiazolidinone ring as a phosphate mimic, we subjected *R*-(–)-**13y**, *R*-(–)-**39g**, *R*-(–)-**39ah**, and *R*-(–)-**39ao** to detailed kinetic analysis according to Dixon and Lineweaver–Burk and determined inhibitory IC₅₀ values at different substrate concentrations. Thereby we could clearly show that *R*-(–)-**13y**, *R*-(–)-**39g**, *R*-(–)-**39ah**, and *R*-(–)-**39a** with *K_i* values between 0.2 and 0.8 μM are potent and substrate competitive inhibitors, which confirms our hypothesis, that the thiazolidinone ring might indeed serve as a crucial element and binds close to the phosphate binding site (Fig. 4).

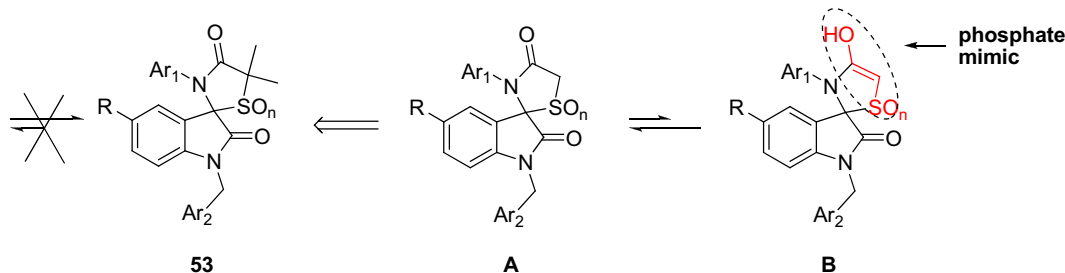


Fig. 4. Tautomerization of spiro-fused indol-2-one-thiazolidinones.

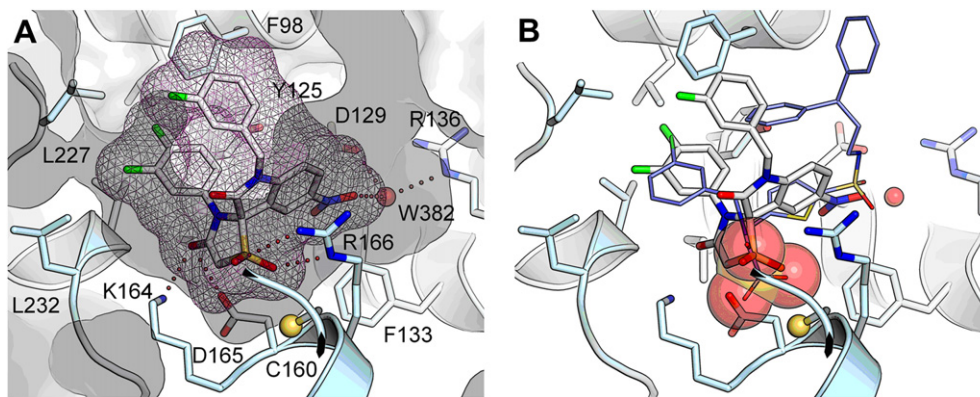


Fig. 5. Proposed binding mode of spiro-fused indol-2-one-thiazolidinone to the active site of MptpB. (A) The *R*-(–)-enantiomer of **13y** was docked to the complex crystal structure of OMTS (**2**) in MptpB. The surface of the protein (white) and the van der Waals radii of the inhibitor (pink colored mesh) indicate good shape complementarity. The proposed binding mode of **13y** indicates the sulfone and the tautomeric oxygen of the thiazolidinone ring within hydrogen bonding distance (red dotted lines) to amino acids of the phosphate binding site (K164, D165, and R166). The oxoindole forms favorable cation– π interactions with the side chain of R166 and the nitro group at the 5-position of the oxoindole core forms water-mediated (W382) hydrogen bonds to the side chains of D129 and R136 and helps to explain why the nitro but not the amine significantly enhances potency against MptpB (Table 1). The dihalogenated anilide and the halogenated *N*-benzyl moiety of the inhibitor are located in a hydrophobic, aromatic sub-pocket flanked by L232, L227, F98, and Y125. (B) Structural alignment of the modeled *R*-(–)-**13y**-MptpB complex with MptpB in complex with phosphate (PDB code: 1YWF) and OMTS (thin blue sticks) (PDB code: 20Z5) shows the sulfone of **13y** and the carboxylate of **2** in a position close to the catalytic cysteine (C160) and isostructural to that of the phosphate (large spheres).

Table 8
Overview of the relative phosphatase activity (%) after addition of the compound (50 μ M), where green fill marks no activity, yellow slight activity, and red is a sign for an active compounds

Cpd.	MptpB	MptpA	PTP1B	SHP-2	PTPN2	h-PTP β	VHR
13y	13	93	92	100	95	85	98
18f	61	90	90	97	86	81	88
39d	72	94	90	86	55	93	80
39g	13	91	94	97	90	108	94
39l	2	88	93	98	82	77	90
39y	28	97	92	100	84	61	87
39ad	19	89	92	90	87	73	82
36b	68	89	93	99	83	78	84
37	52	90	91	96	76	99	81
52a	34	95	98	92	89	72	83
46a	34	92	90	P98	94	77	88
50	50	89	88	94	84	69	95
39ah	8	82	95	76	73	74	83
39aj	41	84	93	81	61	77	68
39ak	27	94	93	80	80	114	71
39al	51	98	87	87	70	74	75
39am	36	97	97	80	79	83	76
39an	1	93	90	85	78	56	75
39ao	24	92	94	79	76	91	87
39ap	76	91	81	74	87	89	75
39aq	30	84	77	69	77	72	72
39ar	55	88	79	78	73	70	66
39as	36	81	78	68	78	68	69
39at	42	93	81	62	80	78	63
39au	21	95	76	75	69	77	72

At least the reversibility, which goes along with the competitive binding mode, marks an important precondition for the development of new, desired antitubercular drugs.

2.9. Molecular modeling studies

To get deeper insights into the possible binding mode of spiro-fused indol-2-one-thiazolidinones in MptpB and to better understand the impact of the configuration of the spiro-center and the 'enol'-form of the thiazolidinone for binding, we used molecular docking. The crystal structures of MptpB in complex with phosphate (PDB code: 1YWF) and an inhibitor (PDB code: 2OZ5) are known from literature and highlight structural elements that are crucial for ligand binding. We docked the 'enol'-form of both enantiomers of **13y** to the rigid protein structure of the inhibitor bound form of MptpB (PDB code: 2OZ5). Only the *R*(-)-enantiomer of **13y** showed a convincing binding mode with direct contacts to amino acids of the active site and an overall good shape complementarity (Fig. 5). The binding mode of *R*(-)-**13y** revealed a number of polar interactions and indicates that the thiazolidinone ring indeed serves as a phosphate mimic.

2.10. Investigation of the selectivity profile of MptpB inhibitors

In order to compare the phosphatase inhibitor selectivity of our newly developed spiro-fused indol-2-one-thiazolidinones, we performed phosphatase profiling for the 25 most potent inhibitors against a panel of six different phosphatases including MptpA, PTP1B, SHP-2, PTPN2, h-PTP β , VHR and measuring the remaining enzyme activity at a concentration of 50 μ M (Table 8). Of particular interest was the finding that all tested compounds showed excellent selectivity in favor of MptpB.

3. Conclusion

In conclusion, indolin-2-on-3-spirothiazolidinones were identified as a novel class of potent and selective MptpB inhibitors. Detailed structure–activity relationship (SAR) studies revealed that a nitro-substituted 2-oxindole core, a dihalogenated anilide moiety, and a halogenated *N*-benzyl fragment are essential for strong inhibitory activity against MptpB. Introduction of the carboxyl function into the thiazolidinone ring led to significant improvement of the solubility and cell permeability of compounds without affecting the inhibitory activity. It was found that the configuration of the spiro-center plays a crucial role for the inhibitory activity against MptpB, *R*(-)-enantiomers are active in the nanomolar range, and are generally 10–20 times more potent than the corresponding *S*(+)-antipodes. In addition, synthesis of structural analogues and extensive kinetic studies showed that (a) the indolin-2-on-3-spirothiazolidinones are reversible and competitive MptpB inhibitors and (b) the 'enol'-form of the thiazolidinone ring is involved in hydrogen bonding with the enzyme. Modeling studies indeed suggested that the *R*(-)-enantiomer fits best to the active site of MptpB and that the thiazolidinone ring system serves as a phosphomimic. Finally, all identified MptpB inhibitors showed excellent selectivity against a panel of other protein tyrosine phosphatases, including MptpA, PTP1B, SHP-2, PTPN2, h-PTP β , and VHR. Consequently, indolin-2-on-3-spirothiazolidinones may be a promising starting point for the development of novel antibiotic agents with activity against *M. tuberculosis*.

4. Experimental

4.1. Chemistry

Unless otherwise noted, all reagents and solvents were purchased from Acros, Fluka, Sigma, Aldrich or Merck and used without

further purification. *m*CPBA was purified according to the reported procedure. Dry solvents were purchased as anhydrous reagents from commercial suppliers. ^1H and ^{13}C NMR spectra were recorded on a Bruker Avance DRX 400 spectrometer at 400 MHz and 100 MHz, respectively. ^1H chemical shifts are reported in δ (ppm) as s (singlet), d (doublet), dd (doublet of doublet), t (triplet), q (quartet), m (multiplet) and br s (broad singlet) and are referenced to the residual solvent signal: CDCl_3 (7.26), $\text{DMSO}-d_6$ (2.50). ^{13}C spectra are referenced to the residual solvent signal: CDCl_3 (77.0) or $\text{DMSO}-d_6$ (39.0). All final compounds were purified to >95% purity, as determined by high-performance liquid chromatography (HPLC). Purity was measured using Agilent 1200 Series HPLC systems with UV detection at 210 nm (System: Agilent Eclipse XDB-C18 4.6 \times 150 mm, 5 μ M, 10–100% CH_3CN in H_2O , with 0.1% TFA, for 15 min at 1.0 mL/min). High resolution electrospray ionization mass spectra (ESI–FTMS) were recorded on a Thermo LTQ Orbitrap (high resolution mass spectrometer from Thermo Electron) coupled to an 'Acela' HPLC System supplied with a 'Hypersil GOLD' column (Thermo Electron). Analytical TLC was carried out on Merck 60 F $_{245}$ aluminum-backed silica gel plates. Compounds were purified by column chromatography using Baker silica gel (40–70 μ m particle size). Melting points were determined using a Büchi Melting Point B-540 and are uncorrected. Preparative chiral HPLC was conducted on a Dionex HPLC system (UltiMate 3000 preparative) with a CHIRALPAK $^{\text{®}}$ IC column (cellulose tris(3,5-dichlorophenylcarbamate) immobilized on 5 μ m silica gel) and *iso*-hexane/ CH_2Cl_2 /EtOH, 60:39.2:0.8 as an eluent and monitored by UV at $\lambda=254$ nm. Circular dichroism spectra were recorded on a JASCO J-815 CD spectropolarimeter using 5 mm cuvette made from Quartz SUPRASIL $^{\text{®}}$.

4.1.1. General procedure for the preparation of *N*-alkyl isatins **11, **16**, **17**, and **25–28** (method A).** NaH (60% dispersion in mineral oil, 240 mg, 6.0 mmol) was added to a solution of isatin **10**, **23b** or **24a** (5.00 mmol) in DMF (25 mL) at 0 $^{\circ}\text{C}$. The mixture was stirred for 10 min at 0 $^{\circ}\text{C}$ and then the corresponding benzyl bromide or alkyl halide (5.25 mmol) was added. The mixture was stirred at room temperature for 8 h and then poured into 120 mL of ice cold water whereupon an orange (brown) solid precipitates. The solid was filtered, washed with water, and dried in vacuo. The crude material was recrystallized from MeOH or purified by column chromatography on silica gel (CH_2Cl_2 /MeOH, 98:2) to provide the corresponding *N*-alkyl isatin.

4.1.2. General procedure for the preparation of indolin-2-on-3-spirothiazolidinones **12, **16**, **17**, **31–35**, and **54** (method B).**

4.1.2.1. Synthesis of isatin-3-imine. A mixture of substituted isatin (0.3 mmol) and the appropriate aromatic amine (0.36 mmol) was refluxed in absolute EtOH (5 mL) for 6 h. EtOH was removed in vacuo and the obtained isatin-3-imine was used directly in the next step.

4.1.2.2. Cyclization into indolin-2-on-3-spirothiazolidinone. A mixture of isatin-3-imine and mercaptoacetic acid (or 2-mercapto-2-methylpropanoic acid) (35 μ L, 0.48 mmol) in 6 mL of absolute toluene was refluxed for 16 h and the water formed was removed by azeotropic distillation. The reaction mixture was cooled, diluted with 20 mL of EtOAc, washed with 1 M aqueous HCl, saturated NaHCO_3 solution, dried over MgSO_4 , and concentrated in vacuo. The crude product was purified by column chromatography on silica gel (CH_2Cl_2 /MeOH, 99:1) to provide corresponding indolin-2-on-3-spirothiazolidinone as an amorphous solid. The resulting sulfides were further oxidized without characterization.

4.1.3. General procedure for the oxidation of indolin-2-on-3-spirothiazolidinones into sulfones **13, **18**, **19**, **36–40**, and **53a** (method C).** To a cooled (0 $^{\circ}\text{C}$) solution of an appropriate sulfide (0.1 mmol) in 3 mL of CHCl_3 was added *m*CPBA (86 mg, 0.5 mmol,

5 equiv). The resulting solution was allowed to reach room temperature and stirred for 24 h. Then the reaction mixture was diluted with 15 mL of EtOAc, washed with 15% NaHSO₃ solution (2×20 mL), saturated NaHCO₃ solution (2×20 mL), dried over MgSO₄, and concentrated in vacuo. The crude product was purified by column chromatography on silica gel (CH₂Cl₂/MeOH, 99:1) to provide the corresponding sulfone as an amorphous solid.

4.1.4. General procedure for the oxidation of indolin-2-on-3-spirothiazolidinones into sulfoxides 14, 41–45, and 53b–d (method D). To a cooled (0 °C) solution of an appropriate sulfide (0.1 mmol) in 3 mL of CHCl₃ was added *m*CPBA (1.1 equiv) and the reaction mixture was stirred at this temperature for 1 h. Then the reaction mixture was diluted with 15 mL of EtOAc, washed with saturated NaHCO₃ solution (2×20 mL), dried over MgSO₄, and concentrated in vacuo. The crude product was purified by column chromatography on silica gel (CH₂Cl₂/MeOH, 98:2) to provide the corresponding sulfoxide as an amorphous solid.

4.1.5. General procedure for the preparation of amides 21a–d (method E). To a solution of acid **20** (42 mg, 0.1 mmol, 1 equiv) in dry DMF (1.5 mL) were added an appropriate aliphatic amine (0.2 mmol, 2 equiv), HBTU (76 mg, 0.2 mmol, 2 equiv), HOBT (27 mg, 0.2 mmol, 2 equiv), and *N,N*-diisopropylethylamine (136 μL, 0.8 mmol, 8 equiv). After the mixture was stirred at room temperature for 4 h, H₂O (5 mL) was added and the obtained emulsion was extracted with EtOAc (3×15 mL). The combined organic layers were washed with saturated NaHCO₃ solution (20 mL), dried over MgSO₄, filtered, and concentrated in vacuo. The residue was purified by flash chromatography (CH₂Cl₂/MeOH, 98:2→97:3) to give the corresponding amide as a colorless amorphous solid.

4.1.6. General procedure for the preparation of tert-butyl esters 30 (method F).

4.1.6.1. Demethylation of 5-methoxy isatin. A solution of an appropriate isatin **27** (4 mmol) in CH₂Cl₂ (20 mL) was treated with BBr₃ (8.0 mL, 1.0 M in CH₂Cl₂, 8.0 mmol, 2 equiv) at –5 °C. The reaction was stirred for 2 h at 0 °C before a saturated solution of NaOAc (25 mL) was added. After separation of the layers, the aqueous phase was extracted twice with CH₂Cl₂ (2×25 mL). The combined organic layers were washed with H₂O, saturated NaCl solution, dried over MgSO₄, filtered, and concentrated in vacuo. Flash chromatography (CH₂Cl₂/MeOH, 97:3→19:1) afforded phenol **29** as an orange amorphous solid.

4.1.6.2. Alkylation of phenol 29 with tert-butyl bromoacetate. NaH (60% dispersion in mineral oil, 144 mg, 3.6 mmol) was added to a solution of phenol **29** (3.00 mmol) in DMF (10 mL) at 0 °C. The mixture was stirred for 10 min at 0 °C and then *tert*-butyl bromoacetate (0.53 mL, 3.3 mmol) was added. The mixture was stirred at room temperature for 3 h and then poured into 50 mL of ice cold water. The obtained emulsion was extracted twice with EtOAc (2×50 mL). The combined organic layers were washed with H₂O, saturated NaCl solution, dried over MgSO₄, filtered, and concentrated in vacuo. Flash chromatography (CH₂Cl₂/MeOH, 98:2) afforded *tert*-butyl ester **30** as an orange amorphous solid.

4.1.7. General procedure for the deprotection of tert-butyl esters 40 and 45 (method G). To a cooled (0 °C) solution of *tert*-butyl ester **40** or **45** (0.1 mmol) in 1 mL of dry CH₂Cl₂ was added 1 mL of TFA. The reaction mixture was stirred at 0 °C for 2 h and all volatiles were removed in vacuo. The crude product was purified by column chromatography on silica gel (CH₂Cl₂/MeOH/HOAc, 95:5:0.5) to provide the corresponding acid as a colorless amorphous solid.

4.1.8. General procedure for the preparation of derivatives 49 (method H). To a solution of amine **48** (24 mg, 0.05 mmol, 1 equiv)

in dry pyridine (1 mL) was added an appropriate acid chloride (0.075 mmol). After the mixture was stirred at room temperature for 4 h, H₂O (5 mL) was added and the obtained emulsion was extracted with EtOAc (3×10 mL). The combined organic layers were washed with saturated NaHCO₃ solution (15 mL), dried over MgSO₄, filtered, and concentrated in vacuo. The residue was purified by flash chromatography (CH₂Cl₂/MeOH, 97:3) to give amide **49** as a colorless amorphous solid.

4.1.9. General procedure for the preparation of acids 52 (method I).

4.1.9.1. Synthesis of indolin-2-on-3-spirothiazolidinones 51. A mixture of substituted isatin **28** (0.3 mmol) and 3,4-difluoroaniline (37 μL, 0.36 mmol) was refluxed in absolute EtOH (5 mL) for 6 h. EtOH was removed in vacuo and the obtained isatin-3-imine was redissolved in 10 mL of absolute toluene. Mercaptosuccinic acid (74 mg, 0.48 mmol) was added to the obtained solution and the reaction mixture was refluxed for 16 h with azeotropic removal of water. The reaction mixture was cooled to room temperature, diluted with 20 mL of EtOAc, washed with 1 M aqueous HCl (2×20 mL), water (2×20 mL), brine (2×20 mL), dried over MgSO₄, and concentrated in vacuo. The crude product was purified by column chromatography on silica gel (CH₂Cl₂/MeOH/HOAc, 95:5:0.5) to provide corresponding acid **51**, which was used directly in the next step.

4.1.10. Oxidation of acid 51 into the corresponding sulfone 52. A mixture of acid **51** (0.2 mmol) and Oxone[®] (2KHSO₄·KHSO₄·K₂SO₄; 738 mg, 1.2 mmol) in 50% methanol/water (20 mL) was stirred at room temperature for 24 h. The reaction mixture was concentrated under reduced pressure to dryness, and the residue was taken up in EtOAc (30 mL). The ethyl acetate layer was washed with 5% citric acid solution (2×15 mL), water (2×15 mL), and brine (2×15 mL) before drying over sodium sulfate. The filtrate was concentrated under reduced pressure and the residue was purified by flash chromatography (CH₂Cl₂/MeOH/HOAc, 95:5:0.5) to give acid **52** as a colorless amorphous solid.

4.2. Proteinbiochemistry

4.2.1. Phosphatase expression and purification. MptpA/B, h-PTPβ, VHR, SHP-2, and PTP1B were cloned, expressed, and purified as recently described.^{17–19} GST-labeled phosphatase PTPN2 was purchased from Stratagene (Amsterdam, NL).

4.2.2. Kinetic assays for IC₅₀ and K_i determinations.

4.2.2.1. MptpB inhibition assay/IC₅₀ determination. *M. tuberculosis* protein tyrosine phosphatase B was dissolved in 25 mM HEPES/50 mM NaCl/Na₂×EDTA 2.5 mM/NP-40 0.025%/DTE 2 mM/1% DMSO buffer at a concentration of 50 nM. Kinetic analysis at 37 °C using the substrate 4-nitrophenol phosphate at pH 7.2 and monitoring the increase of *p*-NP (4-Nitrophenol) at 405 nm gave *K_M* and *K_{cat}* values of (2.3±0.3) mM and 5 s⁻¹ (*K_{cat}*/*K_M*=2300 s⁻¹ M⁻¹). The reaction volume was 100 μL. The reaction was started by the addition of *p*-nitrophenol phosphate (20 mM stock solution, 10 μL) to 90 μL of a solution containing MptpB (preincubated with inhibitor for 15 min). A Tecan Infinite[®] 200 plate reader was used to measure the absorbance of the samples at 405 nm. The reaction velocity was determined from the slope of the absorbance change at 405 nm and related to control values in the absence of the inhibitor. IC₅₀ values were calculated from linear extrapolations of reaction velocity as a function of the logarithm of the concentration. All IC₅₀ values were calculated from at least three independent determinations. The dissociation constant *K_i*, as well as the differentiation between competitive and non-competitive inhibition were determined using the method described by Dixon.²⁰

4.2.2.2. *MptpA*, *PTP1B*, *SHP-2*, *PTPN2*, *h-PTP β* , *VHR* inhibition assay. All buffered solutions contained 2 mM DTE (added on the day of the experiment from 200 mM stock) and the detergent NP-40 (0.025% v/v). The buffers consisted of Tris (50 mM), NaCl (50 mM), and EDTA (0.1 mM) in the case of *h-PTP β* ; HEPES (25 mM), NaCl (50 mM), and EDTA (2.5 mM) in the case of *PTP1B*, *PTPN2*, *MptpA*, and *SHP-2*; and MOPS (25 mM) and EDTA (5 mM) in the case of *VHR*. The final concentration of the enzymes was 1.6 μ g/mL (*PTP1B*), 0.7 μ g/mL (*PTPN2*), 5.0 μ g/mL, 180 nM (*MptpA*), 10.0 μ g/mL (*SHP-2*), 0.13 μ g/mL (*h-PTP β*), and 15.6 μ g/mL (*VHR*). Each reaction was performed in triplicate from identical manual dilutions.

4.3. Molecular modeling

Docking studies were performed using the Schrödinger software package.²¹ The receptor was prepared with the Protein Preparation Wizard and ligands were docked using Glide in XP mode without any constraints.^{22,23} Following settings differed from the default parameters. For H-bond assignment using exhaustive sampling the ligands from the crystal structure and surrounding waters were kept. Finally, two important waters were kept for receptor grid generation. For the latter, the ligand diameter midpoint box was enlarged to 12 \times 12 \times 12 Å. Figures were prepared with PYMOL (www.pymol.org).²⁴

Acknowledgements

This research was supported by the Max-Planck-Gesellschaft, the Fonds der Chemischen Industrie, and the German Federal Ministry for Education (Grant No. BMBF 01GS08102).

Supplementary data

Experimental procedures, analytical data and biochemical evaluation of the binding mode of indolin-2-on-3-spirothiazolidinones. Supplementary data associated with this article can be found in online version at doi:10.1016/j.tet.2011.04.026.

References and notes

- Stewart, G. R.; Robertson, B. D.; Young, D. B. *Nat. Rev. Microbiol.* **2003**, *1*, 97–105.
- Koul, A.; Herget, T.; Klebl, B.; Ullrich, A. *Nat. Rev. Microbiol.* **2004**, *2*, 189–202.
- Singh, R.; Rao, V.; Shakila, H.; Gupta, R.; Khera, A.; Dhar, N.; Singh, A.; Koul, A.; Singh, Y.; Naseema, M.; Narayanan, P. R.; Paramasivan, C. N.; Ramanathan, V. D.; Tyagi, A. K. *Mol. Microbiol.* **2003**, *50*, 751–762.
- (a) Beresford, N. J.; Mulhearn, D.; Szczepankiewicz, B.; Liu, G.; Johnson, M. E.; Fordham-Skelton, A.; Abad-Zapatero, C.; Cavet, J. S.; Tabernero, L. J. *Antimicrob. Chemother.* **2009**, *63*, 928–936; (b) Zhou, B.; He, Y.; Zhang, X.; Xu, J.; Luo, Y.; Wang, Y.; Franzblau, S. G.; Yang, Z.; Chan, R. J.; Liu, Y.; Zheng, J.; Zhang, Z. Y. *Proc. Natl. Acad. Sci. U.S.A.* **2010**, *107*, 4573–4578.
- For recent reviews see: (a) Vintonyak, V. V.; Waldmann, H.; Rauh, D. *Bioorg. Med. Chem.* **2011**, *19*, 2145–2155; (b) Vintonyak, V. V.; Antonchick, A. P.; Rauh, D.; Waldmann, H. *Curr. Opin. Chem. Biol.* **2009**, *13*, 272–283; (c) Bialy, L.; Waldmann, H. *Angew. Chem., Int. Ed.* **2005**, *44*, 3814–3839.
- (a) Nören-Müller, A.; Reis-Correa, I., Jr.; Prinz, H.; Rosenbaum, C.; Saxena, K.; Schwalbe, H. J.; Vestweber, D.; Cagna, G.; Schunk, S.; Schwarz, O.; Schiewe, H.; Waldmann, H. *Proc. Natl. Acad. Sci. U.S.A.* **2006**, *103*, 10606–10611; (b) Correa, I. R., Jr.; Nören-Müller, A.; Ambrosi, H. D.; Jakupovic, S.; Saxena, K.; Schwalbe, H.; Kaiser, M.; Waldmann, H. *Chem.—Asian. J.* **2007**, *2*, 1109–1126.
- Grundner, C.; Perrin, D.; Hooft van Huijsduijnen, R.; Swinnen, D.; Gonzalez, J.; Gee, C. L.; Wells, T. N.; Alber, T. *Structure* **2007**, *15*, 499–509.
- Soellner, M. B.; Rawls, K. A.; Grundner, C.; Alber, T.; Ellman, J. A. *J. Am. Chem. Soc.* **2007**, *129*, 9613–9615.
- Tan, L. P.; Wu, H.; Yang, P. Y.; Kalesh, K. A.; Zhang, X.; Hu, M.; Srinivasan, R.; Yao, S. Q. *Org. Lett.* **2009**, *11*, 5102–5105.
- Vintonyak, V. V.; Warburg, K.; Kruse, H.; Grimme, S.; Hübel, K.; Rauh, D.; Waldmann, H. *Angew. Chem., Int. Ed.* **2010**, *49*, 5902–5905.
- Koch, M. A.; Wittenberg, L. O.; Basu, S.; Jayaraj, D. A.; Gourzoulidou, E.; Reinecke, K.; Odermatt, A.; Waldmann, H. *Proc. Natl. Acad. Sci. U.S.A.* **2004**, *101*, 16721–16726.
- Koch, M. A.; Schuffenhauer, A.; Scheck, M.; Wetzel, S.; Casaulta, M.; Odermatt, A.; Ertl, P.; Waldmann, H. *Proc. Natl. Acad. Sci. U.S.A.* **2005**, *102*, 17272–17277.
- Zhou, L.; Liu, Y.; Zhang, W.; Wei, P.; Huang, C.; Pei, J.; Yuan, Y.; Lai, L. *J. Med. Chem.* **2006**, *49*, 3440–3443.
- Lu, Y.; Shi, T.; Wang, Y.; Yang, H.; Yan, X.; Luo, X.; Jiang, H.; Zhu, W. *J. Med. Chem.* **2009**, *52*, 2854–2862.
- It was found that oxidation of sulfides **51** with 6 equiv of oxone[®] in the MeOH/H₂O (1:1) mixture resulted in formation of one major diastereomer **52**.
- Avdeef, A. In *Pharmacokinetic Optimization in Drug Research*; Testa, B., van de Waterbeemd, H., Folkers, G., Guy, R., Eds.; Helvetica Chimica Acta, Zürich and Wiley-VCH: Weinheim, 2001; pp 305–326.
- Koul, A.; Choidas, A.; Treder, M.; Tyagi, A. K.; Drlica, K.; Singh, Y.; Ullrich, A. *J. Bacteriol.* **2000**, *182*, 5425–5432.
- Seibert, S. F.; Eguereva, E.; Krick, A.; Kehraus, S.; Voloshina, E.; Raabe, G.; Fleischhauer, J.; Leistner, E.; Wiese, M.; Prinz, H.; Alexandrov, K.; Janning, P.; Waldmann, H.; Konig, G. M. *Org. Biomol. Chem.* **2006**, *4*, 2233–2240.
- Evdokimov, A. G.; Pokross, M.; Walter, R.; Meikel, M.; Cox, B.; Li, C.; Bechard, R.; Genbauffe, F.; Andrews, R.; Diven, C.; Howard, B.; Rastogi, V.; Gray, J.; Maier, M.; Peters, K. G. *Acta Crystallogr., Sect. D: Biol. Crystallogr.* **2006**, *62*, 1435–1445.
- Copeland, R. A. *Enzymes: A Practical Introduction to Structure, Mechanism, and Data Analysis*; Wiley: New York, NY, 2000.
- Maestro, Version 9.1*; Schrödinger, LLC: New York, NY, 2010.
- Glide, Version 5.5*; Schrödinger, LLC: New York, NY, 2009.
- Friesner, R. A.; Banks, J. L.; Murphy, R. B.; Halgren, T. A.; Klicic, J. J.; Mainz, D. T.; Repasky, M. P.; Knoll, E. H.; Shelley, M.; Perry, J. K.; Shaw, D. E.; Francis, P.; Shenkin, P. S. *J. Med. Chem.* **2004**, *47*, 1739–1749.
- The PyMOL Molecular Graphics System, Version 1.3, Schrödinger, LLC.